



HAL
open science

Low-Power Laser Processing-Based Approach to Plasma Lithography for Cell Micropatterning

Shinji Deguchi, Sho Yokoyama, Yuki Kamei, Tsubasa S Matsui

► **To cite this version:**

Shinji Deguchi, Sho Yokoyama, Yuki Kamei, Tsubasa S Matsui. Low-Power Laser Processing-Based Approach to Plasma Lithography for Cell Micropatterning. *Journal of Bioanalysis & Biomedicine*, 2015, 07, 10.4172/1948-593x.1000128 . hal-04021327

HAL Id: hal-04021327

<https://hal.science/hal-04021327>

Submitted on 9 Mar 2023

HAL is a multi-disciplinary open access archive for the deposit and dissemination of scientific research documents, whether they are published or not. The documents may come from teaching and research institutions in France or abroad, or from public or private research centers.

L'archive ouverte pluridisciplinaire **HAL**, est destinée au dépôt et à la diffusion de documents scientifiques de niveau recherche, publiés ou non, émanant des établissements d'enseignement et de recherche français ou étrangers, des laboratoires publics ou privés.

Low-Power Laser Processing-Based Approach to Plasma Lithography for Cell Micropatterning

Sho Yokoyama^{1,2}, Yuki Kamei¹, Tsubasa S Matsui¹ and Shinji Deguchi^{1*}

¹Department of Nanopharmaceutical Sciences, Nagoya Institute of Technology, Japan

²Present: Department of Mechanical Engineering, Tokai University, Japan

Abstract

Plasma lithography is a technique to space-selectively create hydrophilic surfaces on silicone materials with oxygen plasma treatment. Cells can thus be micropatterned within the modified surfaces, allowing for artificially controlling the geometry of individual cell colonies. Conventional plasma lithography employs a photolithographically microfabricated mask with which the pattern geometry is determined. However, fast on-demand design change to the micropattern may be limited due to the time and cost associated with the sophisticated photolithographic fabrication. Here we attempted to microfabricate a mask for plasma lithography in a novel, quick, low-cost manner. An infrared absorption film was processed using a low-power Nd:YAG laser on an optical microscope to produce a mask of arbitrary pattern geometries. Our experiments indicate that plasma-shielding masks with various geometries are promptly obtained at a spatial resolution of several tens of microns with a laser power of below 200 mW. We demonstrate that cells are indeed micropatterned on functionalized silicone substrates so as to conform to the geometry of the laser-processed mask, thus suggesting the potential of this technique as a low-cost, fast on-demand means for cell micropatterning.

Keywords: Cell micropatterning; MEMS-free micropatterning; Plasma lithography; Laser processing

Introduction

Micropatterning techniques allow spatially selective control of cell adhesive regions [1-3]. Studies using cell micropatterning have provided many important biological findings, which include the mechanisms of the extracellular matrix (ECM)-dependent spindle orientation [4,5], the force-dependent subcellular localizations of cell adhesions [6,7], and the cell morphology-dependent induction of apoptosis [8], differentiation [9], and formation of primary cilia [10]. Micropatterning techniques are thus useful particularly in cell biology studies for revealing molecular mechanisms of mechanosensing functions [1] as well as in tissue engineering, cell-based biosensors, biomedical analysis, and drug screening [11,12].

Plasma lithography is a technique for producing micropatterns by localized substitution of hydrocarbon groups in the composition of silicone surfaces into oxygen-containing ones through treatment with oxygen plasma [13-16]. The spatially selective treatment is achieved using a fabricated mask with microholes of arbitrary geometries. The mask is attached to the surface of materials for cellular substrate to partly block the exposure to the plasma. Thus, plasma lithography consists of the two steps, i.e., the microfabrication of the masks and subsequent localized plasma treatment for functionalization of the substrate. The microfabrication is usually performed for a silicon chip with the photolithography-based micro electro-mechanical systems (MEMS) processing and subsequent pattern transfer into polydimethylsiloxane (PDMS). The MEMS process for chip fabrications consists of several major steps such as photoresist coating and anisotropic etching and requires special facilities such as a clean room [11]. Thus, low-cost, fast on-demand alternatives may be necessary for further prevalence of the use of micropatterns in a variety of biological applications.

Here, we attempted to develop a MEMS-free approach to plasma lithography, which is aimed at minimizing the time and cost. We processed an infrared-cut film by using a low-power Nd:YAG (neodymium:yttrium aluminum garnet) laser on a microscope to

obtain a microfabricated plasma-shielding mask. The surface of silicone materials, used as a cell culture substrate, was functionalized with oxygen plasma through laser-drilled microholes of the mask. Cell adhesive regions were restricted within the hydrophilized surfaces by inhibiting protein adsorption to the originally hydrophobic, unaltered surfaces. Because design change to micropattern geometries is promptly achieved with the present method, this laser processing-combined plasma lithography can diversify practical approaches to cell micropatterning.

Materials and Methods

Cell culture

A7r5 rat embryonic aortic smooth muscle cells (CRL1444, ATCC) were cultured in low-glucose (1 g/L) DMEM (Gibco) supplemented with 10% fetal bovine serum (SAFC Biosciences) and 1% penicillin-streptomycin (Wako). Cells were maintained in a 5% CO₂ incubator at 37°C.

Laser processing

Infrared absorption films (Purecut 89 plus, 3M) of a size of 18 × 18 mm² were attached to the surface of a cover glass (Matsunami; 0.12 mm in thickness). This film is transparent in appearance so that it is available on an optical microscope. The film consists of two layers (25 μm in total thickness), i.e., one for self-adhesion and the other for infrared absorption. The cover glass supporting the adhesive film was fixed on the stage of an inverted microscope (IX-71, Olympus)

*Corresponding author: Shinji Deguchi, Gokiso, Showa, Nagoya 466-8555, Japan, Tel: +81 52 735 5178; E-mail: deguchi@nitech.ac.jp

Received April 30, 2015; Accepted May 18, 2015; Published May 21, 2015

Citation: Yokoyama S, Kamei Y, Matsui TS, Deguchi S (2015) Low-Power Laser Processing-Based Approach to Plasma Lithography for Cell Micropatterning. J Bioanal Biomed 7: 081-086. doi:10.4172/1948-593X.1000128

Copyright: © 2015 Yokoyama S, et al. This is an open-access article distributed under the terms of the Creative Commons Attribution License, which permits unrestricted use, distribution, and reproduction in any medium, provided the original author and source are credited.

equipped with an Nd:YAG laser generator (Sigma Koki; 1,064 nm in wavelength, 2.5 W in the maximum power). According to the manufacturer's specifications, the film absorbs 76% of the infrared light in the wavelength range of 780-2,500 nm. Thus, the laser is used as a heat source to ablate a small area of the film focused through an objective lens (20X, NA=0.45 or 40X, NA=0.75; UPlanFL, Olympus). The position of the film was altered using a manual xy stage during processing so as to finally have a microhole with a shape of "+" (plus) or "-" (minus) (Figure 1). In a separate experiment, the actual laser intensity was measured above the objective lens through the cover glass using an optical power meter (ADCE8230E+11, Advantest).

Substrate functionalization

The surface of a 35 mm polystyrene tissue culture dish (Iwaki) was coated using a spin-coater with a PDMS prepolymer (Sylgard 184, Dow Corning Toray), which was prepared according to the manufacturer's instruction; i.e., the prepolymer was mixed at 10:1 weight ratio of base agent to curing agent, stirred, degassed using a vacuum, and poured onto the dish (0.2 g in weight for each dish) at room temperature (Figure 1). The PDMS coated on the dish was then oven cured at 60°C for 800 min. The laser-processed infrared-cut film was self-attached to the surface of the PDMS. The dish supporting the film on the PDMS-coated surface was then placed on the lower electrode of a direct-current-driven plasma generator (SEDE-P, Meiwafofosis). The surface of the dish was treated with oxygen plasma (4 mA in current, 20 Pa in pressure) for 3 min. After careful removal of the film by forceps, the surface was treated with 0.2% Pluronic F-127 (Invitrogen) for 1 h and then coated with 0.1% gelatin (Sigma) in PBS for 1 day at 37°C, which was afterwards followed by the seeding of A7r5 cells.

Microscopy

75 µg/ml Alexa 488-conjugated fibrinogen (Molecular Probes) was coated on the substrate for 1 h at 4°C prior to the cell seeding. Fluorescence images were taken using a camera (ORCA-R2, Hamamatsu) under a microscope (IX-71, Olympus). Cells were then plated on the substrate at a density of 6×10^3 cells/cm² and observed with phase-contrast microscopy using a camera (Moticam 1000, Motic)

under a microscope (CKX41, Olympus) at 24 h after cell seeding. Laser processing was also observed in real-time at 30 Hz by using an infrared video camera (XC-EI50, Sony).

Image analysis

The spatial accuracy of the present micropatterning was evaluated based on the following image analysis. The hole-lengths of the laser-processed microholes as well as the lengths of corresponding fluorescent fibrinogen micropatterns and cell colonies were measured using ImageJ (NIH). The length ratio of fibrinogen micropattern to microhole and that of cell colony to microhole were quantified; thus, the ratio should be unity if the size of fibrinogen micropattern, which favors to adhere to hydrophilic regions, is identical to that of the microhole although the microhole-cell colony ratio may be affected by the active migratory behavior of the cells.

Reusability of infrared absorption films

Repeatability of the cell patterning effect using identical laser-processed films was investigated to assess their durability. An infrared-cut film was processed with the infrared laser so as to have a "minus"-shaped hole and used as a plasma-shielding mask for plasma lithography followed by the cell plating. The same procedure of the plasma lithography and subsequent cell plating was conducted repeatedly 18 times for different PDMS-coated polystyrene dishes using the same film. The film and cells were observed with microscopy to examine if the film is sufficiently durable even after the successive uses to allow cells to align in an identical manner on different substrates. Here, for cell colony measurement, we quantified the width ratio of cell colonies to the microholes in the direction of the short axes. The width was measured along the cell colony where cells were well spread out.

Results

Microholes are created in films by low-power laser processing

First, we measured the relationship between the laser intensity that displayed on the laser device panel and that actually measured above the cover glass on the objective lens. A linear regression curve was

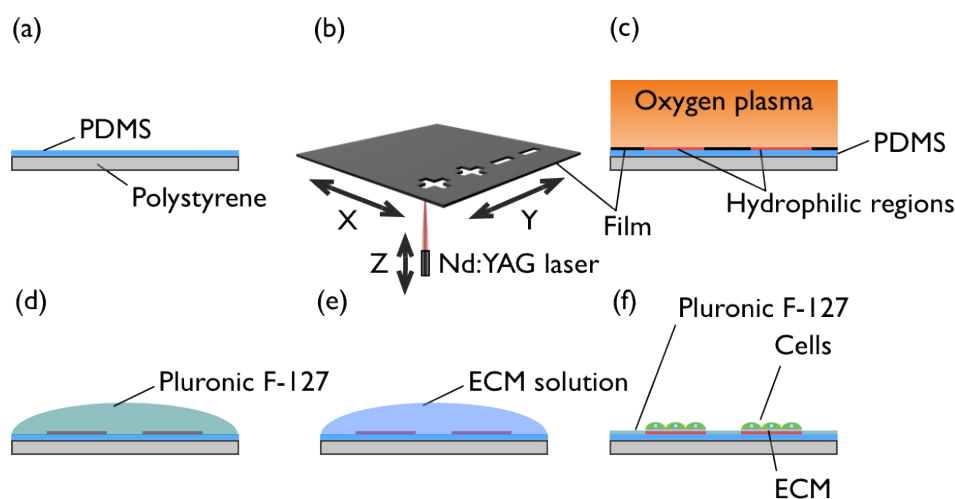


Figure 1: Schematic of the procedure for creating cell micropatterns. Polystyrene dishes are coated with PDMS (a). Separately, infrared absorption films are processed by a low-power Nd:YAG laser on an inverted microscope to remove a small part of the film by melt ejection (b). The PDMS-coated substrates are treated with oxygen plasma, through the laser-processed film as a plasma-shielding mask that is brought into contact with the substrates, to locally form oxygen-rich hydrophilic regions at the surface (c). The substrates after the removal of the mask were treated with Pluronic F-127 (d) and then ECM (gelatin) (e). ECM and cells adhere preferentially to the plasma-treated regions (f).

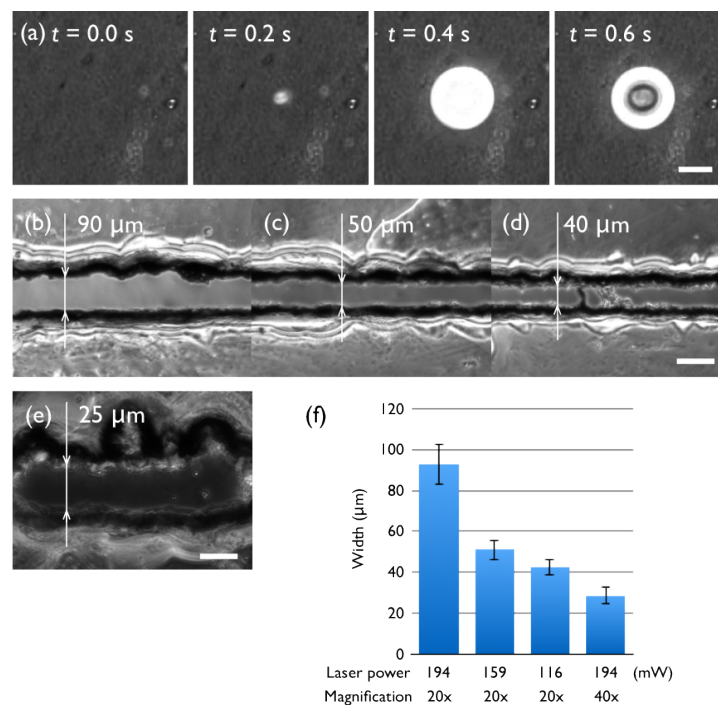


Figure 2: Representative phase-contrast images of microholes created in the infrared absorption films with different Nd:YAG laser powers and objective lens magnifications. (a) 159 mW, 20X. The film before ($t=0.0$ s) and after ($t=0.2$ s) the initiation of the laser irradiation, taken by the infrared video camera. The film during heat absorption as indicated by a bright intensity ($t=0.4$ s), in which a microhole is not yet created. The film after the creation of a microhole as indicated by a decrease in the light intensity at the center ($t=0.6$ s) where the infrared absorption film is melt ejected. (b–e) Linear microholes created at 194 mW, 20X (b), 159 mW, 20X (c), 116 mW, 20X (d), and 194 mW, 40X (e). (f) Quantification of the widths of the microholes, represented by mean \pm SD ($n=12$). Scale bars, 100 μ m (a–d); 20 μ m (e).

obtained from the average data (data not shown), and hereafter this calibration data was used to describe the output of the laser.

The laser was focused on an infrared film attached to the cover glass at various magnitudes of power and different magnifications of the objective lens. Local removal of the film by melt ejection was realized at the focus particularly by increasing the power of the laser, but we tried to drill as small holes as possible by lowering the power to test the spatial resolution of the processing. Here we processed a part of the 18 mm \times 18 mm film just to demonstrate the feasibility of the infrared film as a plasma-shielding mask. The time required to drill a microhole depends substantially on how fast the stage supporting the film is moved within the same plane as the microhole is created in the film quickly (<1 s) upon absorption of the infrared laser (Figure 2a). We found that increasing the magnification of the objective lens also resulted in the production of a smaller microhole. We then demonstrated that linear holes with a width of, on average, 25 μ m were created at a laser power of 194 mW and an objective magnification of 40X by manually displacing the position of the focus within the xy plane (Figures 2b–2e). At a low magnification of 20X, microholes with a width of \sim 40 μ m were created even with a low laser power of 116 mW. It was often hard to stably yield a constant-width microhole because of the difficulty in manually focusing the identical plane at a high magnification. In addition, prolonged laser absorption gradually enlarged the processed area within the film probably due to accumulation of the heat. Because of these deviations from the focus and the more or less time-dependent changes in the affected areas, wavy burrs were inevitably produced along the edges of the microholes. We then quantified the variations in the width of the processed linear microholes as the standard deviation (Figure 2f).

Proteins/cells adhere to the substrate according to the microhole geometry

Next, we performed plasma lithography using the laser-processed film as a plasma-shielding mask. Because the thin film inherently consists of two sub-layers aimed at increasing adhesion as well as infrared absorption, it is capable of self-attaching to the PDMS-coated substrate. Even with a slight gap between the mask and substrate, plasma can partly diffuse into the gap under the direct-current-driven plasma generation [15]. Because the partial diffusion consequently results in ill-defined micropatterns, the firm attachment between the self-adhesive mask and substrate is suitable for plasma lithography-based micropatterning. Oxygen plasma treatment was then performed to the PDMS surface through the mask, which was followed by Pluronic treatment for protein inhibition and hydrophilization for hydrophobic regions and also ECM coating (i.e., gelatin). For visualization of protein/cell adhesive regions, fluorescent fibrinogen and cells were plated, and we investigated whether their micropatterns conform to the mask geometries. We demonstrated the conformity using a “plus”-shaped mask with which cells and proteins exhibited similar micropatterns (Figure 3a). Quantification of the conformity shows that ECM (i.e., fibrinogen) was basically confined within the mask configuration as it preferentially adheres to the protein adhesive regions (Figures 3b and 3c). Cells in general actively spread or shrink their peripheral lamellipodia, and cells also interact with neighboring cells [17]; these behaviors may perturb the outline of the cell colonies. Indeed, we observed a bridging of adjacent cells at the originally crossed portion of the “plus”-shaped micropattern (Figure 3a, Cells). We also found non-specific adhesion of fibrinogen to the outside of the desired “plus”-

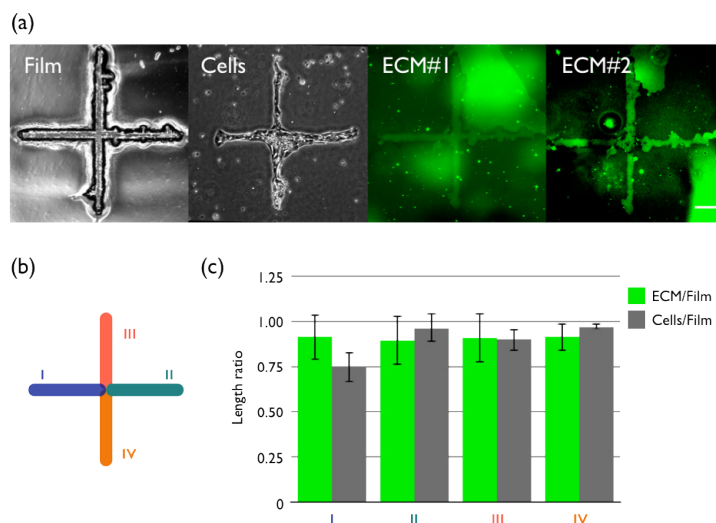


Figure 3: Representative images of spatially selective cell adhesions by the laser-processed mask-based plasma lithography. (a) A “plus”-shaped microhole opened in an infrared absorption film (Film; phase-contrast) allows cells (Cells; phase-contrast) to selectively adhere to the unmasked regions although non-specific adhesion of fibrinogen was partly observed; here, two representative images are shown (ECM#1, #2; fluorescence). (b) Regions for evaluation of patterning accuracy. (c) The length ratios measured at the different regions (I to IV) shown in (b), represented by mean \pm SD ($n=3$). Scale bar, 200 μ m.

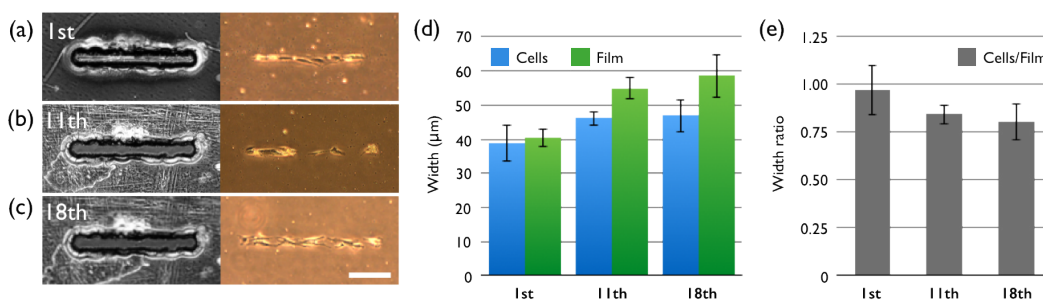


Figure 4: Durability of the infrared absorption film as a plasma-shielding mask. (a) Initial phase-contrast images of a rectangular microhole created in a film (left) and a resulting cell colony formed within the “minus”-shaped microdomain (right). (b, c) The same mask as of that in (a) but after 11 (b) or 18 (c) times repeated use (left). Cells faithfully adhere to the specific area (right), thus showing the repeatable use of the identical mask. (d) Widths of cell colonies (Cells) and microholes (Film) after 1, 11 and 18 times use, represented by mean \pm SD ($n=6$). (e) Width ratio of cell colony to microhole, represented by mean \pm SD ($n=6$). Scale bar, 200 μ m.

shaped region when we repeated these experiments several times (Figure 3a, ECM#1, #2). The place of the ECM non-specific adhesions varied from experiment to experiment for some reason. The reason of the non-specific adhesion was unclear, but we confirmed that cells were nevertheless consistently present within the desired region.

The plasma-shielding mask is reusable

For practical use, it is expected that the thin films are mechanically durable enough to be repeatedly applied to plasma lithography; otherwise, the film may produce inaccurate micropatterns due to its mechanical distortion or breakage and thus has to be expendable. We tested the durability using a mask with a “minus”-shaped microhole and found that similar linear micropatterns of cells are created as many times as needed; at least, we confirmed the reusability of the same film as a plasma-shielding mask even after 18-times use (Figures 4a-4c). We quantified the change in the feature size and found that particularly the microhole was enlarged in the short axis after use because the

laser processed inner edges or burrs are partly removed (Figure 4d). Consequently, the width ratio of cells to film reduced, but the partial removal of the burrs occurs only in the beginning of the use (Figures 4d and 4e). Thus, the microhole features as well as the width ratio become unchanged after several uses.

Discussion

Plasma lithography is a practical option for conducting cell micropatterning in which a plasma-shielding mask having microholes or microfeatures of desired shapes is used to spatially restrict originally hydrophobic surfaces to be exposed to oxygen plasma for functionalization [13-16]. The remaining hydrophobic regions are treated with protein-resistant chemicals such as Pluronic F-127. Protein/cell adhesive regions can thus be selectively confined, thereby allowing for control of localization and morphology of cell colonies. For traditional plasma lithography, PDMS-made masks are utilized that are transferred from MEMS-fabricated silicon chips [13-15].

These silicon chips can produce multiple copies of masks, but repeated on-demand design change may be limited because the fabrication is accompanied by a considerable amount of steps such as photoresist coating and anisotropic etching performed in a sophisticated clean room. Alternatively, we previously employed a commercially available electron microscopy grid as a shielding mask [16]; although this approach works successfully, design change to the mask geometry is difficult. In the present study, we instead promptly created plasma-shielding masks from commercially available infrared absorption films by infrared laser processing. A spatial resolution of up to 25 μm was achieved in our setup using a low laser power of below 200 mW. The current approach thus consists of simpler steps of the low-power laser processing and plasma treatment, all of which can be completed in a standard experimental room within several minutes. Given these unique characteristics including the circumvention of the MEMS process, the present technique potentially becomes a practical option for performing cell micropatterning.

Because laser irradiation can be focused to a small area, it is generally suited to perform precise micromachining called laser processing or laser ablation [18]. Laser processing is a thermal process in which the laser is used as a heat source to remove materials by melt ejection. A pulsed laser is normally used for generating up to megawatt-class high power, which is required to process hard materials that are not cut by conventional machining process [18-22]. In laser-based micropatterning techniques that are not aimed at physically drilling the substrate because of their low power, various types of photosensitizers are employed to locally functionalize the substrate upon light excitation [23,24]. However, photosensitizers are in general not very biocompatible, and engineering of photosensitive materials requires dedicated chemistry [1]. In the present study, we introduced a new, straightforward approach realized with a fairly low-power laser to drill not the cell culture substrate directly but a plasma-shielding mask for subsequent plasma lithography. Our strategy is to use an infrared absorption film with a small thickness close to the size of cells but durable enough to be replaced onto the cell substrate. The laser-focused area of the infrared absorption film is promptly removed by melt ejection even with the low-power infrared laser, thus allowing for fine control of processing at a resolution of several tens of microns that is comparable to the size of individual cells.

The line width of the micropatterns that our experimental setup was able to yield was $>25 \mu\text{m}$. The spatial resolution was improved by decreasing the laser power or increasing the magnification of the objective lens, which contribute to focusing of the laser beam and ejecting as small amount of melted portions as possible. For further improvement, automatic focusing and constant-rate planar feed of the film position during laser processing are required, which will be the subject of future investigation. Moreover, the use of a motorized microscope stage is convenient for repeating sequential laser processing and drawing micropatterns of arbitrary geometries although we controlled the film position in a manual manner in the present study.

Conclusion

We described a new approach to plasma lithography-based cell micropatterning without using photolithographically microfabricated masks. We promptly processed a thin infrared absorption film using a low-power infrared laser, and then spatially controlled exposure to oxygen plasma was achieved according to the geometry of the mask in contact with the substrate. Thus, the usefulness of the processed thin film as a plasma-shielding mask was demonstrated. Cells were

then seeded on the surface after the removal of the mask and the subsequent treatments with Pluronic F-127 and ECM. We observed spatially selective adhesions of cells to the artificially confined regions, suggesting that cell adhesive regions with desired geometries are effectively created. Our approach thus enables fast on-demand design change to the geometry of cell micropatterns. Reusability of identical microfabricated masks was also demonstrated. Thus, although motorized stages will be necessary for improving the spatial resolution, this new, adjustable technique independent of the MEMS technology can diversify practical options for performing cell micropatterning.

Acknowledgment

This work was partly supported by JSPS KAKENHI grants (25242039, 26560208, 50638707) from the MEXT of Japan and A-STEP from Japan Science and Technology Agency. Author contributions: SY, TSM, and SD designed the study; SY and YK performed experiments and analyzed data; TSM and SD contributed reagents/materials/tools; and SY and SD wrote the paper.

References

1. Théry M (2010) Micropatterning as a tool to decipher cell morphogenesis and functions. *J Cell Sci* 123: 4201-4213.
2. Ruiz SA, Chen CS (2007) Microcontact printing: A tool to pattern. *Soft Matter* 3: 168-177.
3. Yokoyama S, Matsui TS, Deguchi S (2014) Microcontact peeling as a new method for cell micropatterning. *PLoS One* 9: e102735.
4. Théry M, Racine V, Pépin A, Piel M, Chen Y, et al. (2005) The extracellular matrix guides the orientation of the cell division axis. *Nat Cell Biol* 7: 947-953.
5. Théry M, Jiménez-Dalmaroni A, Racine V, Bornens M, Jülicher F (2007) Experimental and theoretical study of mitotic spindle orientation. *Nature* 447: 493-496.
6. Théry M, Pépin A, Dressaire E, Chen Y, Bornens M (2006) Cell distribution of stress fibres in response to the geometry of the adhesive environment. *Cell Motil Cytoskeleton* 63: 341-355.
7. Deguchi S, Matsui TS, Iio K (2011) The position and size of individual focal adhesions are determined by intracellular stress-dependent positive regulation. *Cytoskeleton (Hoboken)* 68: 639-651.
8. Chen CS, Mrksich M, Huang S, Whitesides GM, Ingber DE (1997) Geometric control of cell life and death. *Science* 276: 1425-1428.
9. McBeath R, Pirone DM, Nelson CM, Bhadriraju K, Chen CS (2004) Cell shape, cytoskeletal tension, and RhoA regulate stem cell lineage commitment. *Dev Cell* 6: 483-495.
10. Pitaval A, Tseng Q, Bornens M, Théry M (2010) Cell shape and contractility regulate ciliogenesis in cell cycle-arrested cells. *J Cell Biol* 191: 303-312.
11. Xia Y, Whitesides GM (1998) Soft lithography. *Annu Rev Mater Sci* 28: 153-184.
12. Kane RS, Takayama S, Ostuni E, Ingber DE, Whitesides GM (1999) Patterning proteins and cells using soft lithography. *Biomaterials* 20: 2363-2376.
13. Goessl A, Bowen-Pope DF, Hoffman AS (2001) Control of shape and size of vascular smooth muscle cells in vitro by plasma lithography. *J Biomed Mater Res* 57: 15-24.
14. Rossi MP, Xu J, Schwarzbauer J, Moghe PV (2010) Plasma-micropatterning of albumin nanoparticles: Substrates for enhanced cell-interactive display of ligands. *Biointerphases* 5: 105-113.
15. Junkin M, Wong PK (2011) Probing cell migration in confined environments by plasma lithography. *Biomaterials* 32: 1848-1855.
16. Deguchi S, Nagasawa Y, Saito AC, Matsui TS, Yokoyama S, et al. (2014) Development of motorized plasma lithography for cell patterning. *Biotechnol Lett* 36: 507-513.
17. Asghar W, Kim YT, Ilyas A, Sankaran J, Wan Y, et al. (2012) Synthesis of nano-textured biocompatible scaffolds from chicken eggshells. *Nanotechnology* 23: 475601.
18. Ghosh A, Mallik AK (2010) *Manufacturing Science*. Affiliated East-west Press.

19. Liu Y, Sun S, Singha S, Cho MR, Gordon RJ (2005) 3D femtosecond laser patterning of collagen for directed cell attachment. *Biomaterials* 26: 4597-4605.
20. Ihlemann J (2008) Micro patterning of fused silica by laser ablation mediated by solid coating absorption. *Appl Phys A* 93: 65-68.
21. Lee SH, Moon JJ, West JL (2008) Three-dimensional micropatterning of bioactive hydrogels via two-photon laser scanning photolithography for guided 3D cell migration. *Biomaterials* 29: 2962-2968.
22. Hook AL, Creasey R, Hayes JP, Thissen H, Voelcker NH (2009) Laser-based patterning for transfected cell microarrays. *Biofabrication* 1: 045003.
23. Itoga K, Yamato M, Kobayashi J, Kikuchi A, Okano T (2004) Cell micropatterning using photopolymerization with a liquid crystal device commercial projector. *Biomaterials* 25: 2047-2053.
24. Perez-Hernandez H, Paumer T, Pompe T, Werner C, Lasagni AF (2012) Contactless laser-assisted patterning of surfaces for bio-adhesive microarrays. *Biointerphases* 7: 35.